Computer Physics Communications 66 (1991) 219–232
North-Holland

A universal solver for hyperbolic equations by cubic-polynomial interpolation
I. One-dimensional solver

T. Yabe
Department of Electronic Engineering, Gunma University, Tenjin-chou 1-5-1, Kiryu, Gunma 376, Japan

and

T. Aoki
Department of Energy Sciences, The Graduate School at Nagatsuta, Tokyo Institute of Technology, 4259 Nagatsuta, Midori-Ku, Yokohama 227, Japan

Received 23 September 1990; in revised form 11 January 1991

A new numerical method is proposed for general hyperbolic equations. The scheme uses a spatial profile interpolated with a cubic polynomial within a grid cell, and is described in an explicit finite-difference form by assuming that both a physical quantity and its spatial derivative obey the master equation. The method gives stable and less diffusive results even without any flux limiter. It is successfully applied to the KdV equation, a one-dimensional shock-tube problem and a cylindrically converging shock wave.

1. Introduction

In previous papers, we proposed a low diffusion and stable algorithm, cubic-interpolated pseudo-particle (CIP) [1–4], for solving general hyperbolic equations. In the method a spatial profile within each grid is interpolated with a cubic polynomial, and both the value f and its spatial derivative ∇f on the grid are predicted in advance. Since the gradient of the quantity is a free parameter, the scheme is completely different from the spline method [5,6]; in the latter method, the gradient is calculated by assuming continuity of the quantity, the first derivative and the second derivative of the quantity at the mesh boundaries, and is independent of the master equation. In contrast, the first derivative in the CIP is calculated from a model equation for the spatial derivative which is consistent with the master equation.

Among the previous CIP schemes, the compact CIP method [3,4] is simple, less diffusive and stable. The method does not use a characteristic speed for wave propagation and hence is quite different from most of the modern schemes [7–9]. However, it can produce good results for many example problems.

In this paper, we reconstruct a one-dimensional CIP solver [3,4] in order to extend the algorithm to nonlinear and multidimensional cases. The extension to higher dimensions will be given in the following paper [15].

2. Basic algorithm – CIP0

Let us first consider a one-dimensional hyperbolic equation:

$$L_1 f \equiv \frac{\partial f}{\partial t} + u\frac{\partial f}{\partial x} = 0. \tag{1}$$

Even if u is a function of t and x, we can locally use the solution

$$f(x_i, t) \sim f(x_i - u\,\Delta t, t - \Delta t), \tag{2}$$

where x_i is the grid point. Since the value of f is given only at grid points $x_1, \ldots, x_i, \ldots$, $f(x_i - u\,\Delta t)$ must be approximated by using these values. In previous CIP schemes [1–4], we have used cubic-polynomial interpolation such as

$$F_i(x) = \left[(a_i X + b_i) X + f_i'\right] X + f_i, \tag{3}$$

where $X = x - x_i$. Here, we use an expression slightly different from the previous one in order to make it a multidimensional solver. If only the values f at all grid points, $f_i (i = 1, \ldots, i_{\max})$, are known, we have three parameters a_i, b_i, $f_i' = \partial_x f_i$ to be determined, where $\partial_x f$ is the abbreviated form of $\partial f/\partial x$. Since conventional spline interpolation requires the continuity of f, $\partial f/\partial x$ and $\partial^2 f/\partial x^2$ at each grid point, matrix equations must be solved in order to determine a, b, and f', even in the one-dimensional case, and are not suitable for efficient computation on vector computers; this becomes a further troublesome problem in multidimensional cases. We have shown in previous one-dimensional CIP [1–4] that the first spatial derivative must be determined consistently with the master equation (see eq. (4)). In this manner, we have obtained quite accurate solutions without solving a matrix equation to determine the polynomial. We will use a similar principle in this paper.

The equation for the first spatial derivative is derived from eq. (1) (that is, from $\partial_x L_1 f = 0$):

$$L_1(\partial_x f) = -\frac{\partial u}{\partial x}\frac{\partial f}{\partial x} \equiv g. \tag{4}$$

If f, $\partial_x f$ at all grid points are given by eqs. (1) and (4), only two conditions are required to determine the coefficients a and b. We require that the value f and the spatial derivative $\partial_x f$ should be continuous at the grid points $i + 1$. As a result, we have

$$a_i = \frac{(f_i' + f_{i+1}')}{\Delta x^2} + \frac{2(f_i - f_{i+1})}{\Delta x^3}, \tag{5}$$

$$b_i = \frac{3(f_{i+1} - f_i)}{\Delta x^2} - \frac{(2f_i' + f_{i+1}')}{\Delta x}. \tag{6}$$

Once a_i and b_i are given in terms of f^n and f'^n, the value of f^{n+1} and f'^{n+1} are simply given by shifting the cubic polynomial as in eq. (2). For a linear advection equation where u = constant eq. (4) is equivalent to eq. (1). Therefore, eq. (2) can also be used in estimating f'^{n+1}. Thus we obtain

$$f_i^{n+1} = F_i(x_i - u\,\Delta t) = \left[(a_i\xi + b_i)\xi + f_i'\right]\xi + f_i, \tag{7}$$

$$f_i'^{n+1} = \mathrm{d}F_i(x_i - u\,\Delta t)/\mathrm{d}x = (3a_i\xi + 2b_i)\xi + f_i', \tag{8}$$

where $\xi = -u\,\Delta t$. This expression is derived for $u < 0$. For $u \geq 0$, we obtain a similar expression by simply replacing Δx by $-\Delta x$ and $i + 1$ by $i - 1$ in eqs. (5) and (6).

It is easy to prove that eqs. (5)–(8) give exactly the same expression as those given in ref. [3,4]. This scheme is called CIP0 hereafter and it is tested for the propagation of square and triangular waves, and these results are shown in fig. 1a.

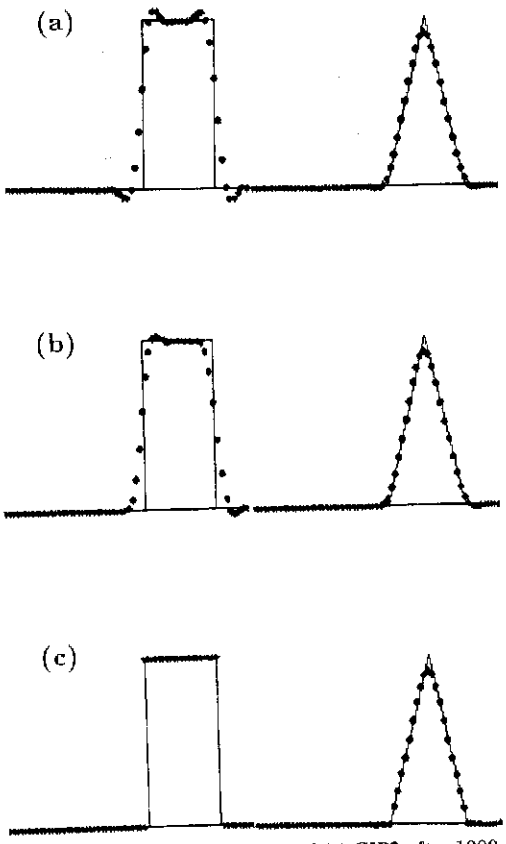

Fig. 1. Linear wave propagation with (a) CIP0, (b) CIP1 and (c) CIP2 after 1000 time steps with $u\,\Delta t/\Delta x = 0.2$.

3. Improved scheme – CIP1

The basic scheme given in section 2 may be sufficient for many purposes including nonlinear problems as will be shown later in this paper. However, it is possible to increase the accuracy at a discontinuity of a square wave. One of the improvements can be done by checking the interpolation scheme, as has been proposed in ref. [3,4]. In this section and the following section, we give an alternative method which improves the ability to treat the discontinuous front.

In this improved scheme, we make a special treatment at the point where the spatial derivative is not continuous. This treatment is reasonable because the scheme in the previous section relies on the continuity of the derivative and it is better modified there. Such a break occurs, for example, at the edge of a square wave. At this discontinuity, the spatial derivative f' should have different values f'_{R} and f'_{L} for the right-hand-sided and left-hand-sided spatial derivatives, respectively. Therefore, eqs. (5) and (8) are rewritten in the present case as

$$a_i = \frac{(f'_{i,\mathrm{R}} + f'_{i+1,\mathrm{L}})}{\Delta x^2} + \frac{2(f_i - f_{i+1})}{\Delta x^3}, \tag{5'}$$

$$b_i = \frac{3(f_{i+1} - f_i)}{\Delta x^2} - \frac{(2f'_{i,\mathrm{R}} + f'_{i+1,\mathrm{L}})}{\Delta x}, \tag{6'}$$

$$f_i^{n+1} = F_i(x_i - u\,\Delta t) = \left[(a_i\xi + b_i)\xi + f'_{i,\mathrm{R}}\right]\xi + f_i, \tag{7'}$$

$$f_i'^{n+1} = \mathrm{d}F_i(x_i - u\,\Delta t)/\mathrm{d}x = (3a_i\xi + 2b_i)\xi + f'_{i,\mathrm{R}}, \tag{8'}$$

where $\xi = -u\,\Delta t$ for $u < 0$. For $u \geq 0$, we obtain a similar expression by simply interchanging the subscripts R and L of f' in eqs. (5′)–(8′) in addition to replacing Δx by $-\Delta x$ and $i+1$ by $i-1$ in eqs. (5′) and (6′) as has already been done in eqs. (5) and (6). In all places except at the discontinuity, $f'_R = f'_L = f'$, and f' is estimated with the master equation as in CIP0. However, at the discontinuity, $f'_R \neq f'_L$ and f' for this case is given below.

In order to indicate the discontinuity, we introduce an index NP_i and we set $NP_i = 0$, except at a discontinuity. The discontinuity may be found by inspecting a value $|f_i - f_{i-1}|/|f_{i+1} - f_i|$, and we define

$$
\begin{aligned}
&NP_i = -1 \quad \text{if} \quad \frac{|f_i - f_{i-1}|}{|f_{i+1} - f_i|} \quad \text{and} \quad \frac{|f_{i-1} - f_{i-2}|}{|f_{i+1} - f_i|} < \epsilon \\
&NP_i = 1 \quad \text{if} \quad \frac{|f_i - f_{i-1}|}{|f_{i+2} - f_{i+1}|} \quad \text{and} \quad \frac{|f_i - f_{i-1}|}{|f_{i+1} - f_i|} \geq \frac{1}{\epsilon}
\end{aligned}
\tag{9}
$$

Here, ϵ should be taken as small as possible ($\epsilon = 0.05$ for example [3,4]). At this discontinuity, f'_R or f'_L will not be determined from the master equation, but will be given by

$$
\begin{aligned}
&f'_{i,L} = \frac{f_i - f_{i-1}}{\Delta x} \quad \text{if} \quad NP_i = -1, \\
&f'_{i,R} = \frac{f_{i+1} - f_i}{\Delta x} \quad \text{if} \quad NP_i = 1.
\end{aligned}
\tag{10}
$$

However, $f'_{i,R}$ at $NP_i = -1$ and $f'_{i,L}$ at $NP_i = 1$ are not subjected to this modification and are given by the master equation as in CIP0. This scheme is called CIP1. The scheme can be written in a compact form if we introduce $GP_{i,1} = f'_R$ and $GP_{i,-1} = f'_L$. Then the scheme for $u < 0$ and $u \geq 0$ is written as

$$
\begin{aligned}
&\textit{set } GP_{i,1} = GP_{i,-1} = f'_i \quad \textit{for} \quad i = 1, \ldots, \text{imax} \\
&\textit{call } \text{NINDEX} \\
&X = -u\,\Delta t \\
&\text{isgn} = -\text{sgn}(u) \\
&FD = \frac{f_{i+\text{isgn}} - f_i}{\Delta x} \times \text{isgn} \\
&a = \frac{GP_{i,\text{isgn}} + GP_{i+\text{isgn},-\text{isgn}} - 2FD}{\Delta x^2} \\
&b = \frac{3FD - 2GP_{i,\text{isgn}} - GP_{i+\text{isgn},\text{isgn}}}{\Delta x} \times \text{isgn} \\
&f_i^{n+1} = \left((aX + b)X + GP_{i,\text{isgn}}\right)X + f_i \\
&f_i'^{n+1} = (3aX = 2b)X + GP_{i,\text{isgn}}
\end{aligned}
\tag{11}
$$

where the subroutine NINDEX is the process given by eqs. (9) and (10). The result with this scheme is given in fig. 1b.

4. Improved scheme – CIP2

The scheme introduced in section 3 can suppress oscillations at the discontinous edge but is still not enough for the propagation of the square wave. This is obvious because the cubic polynomial does not give

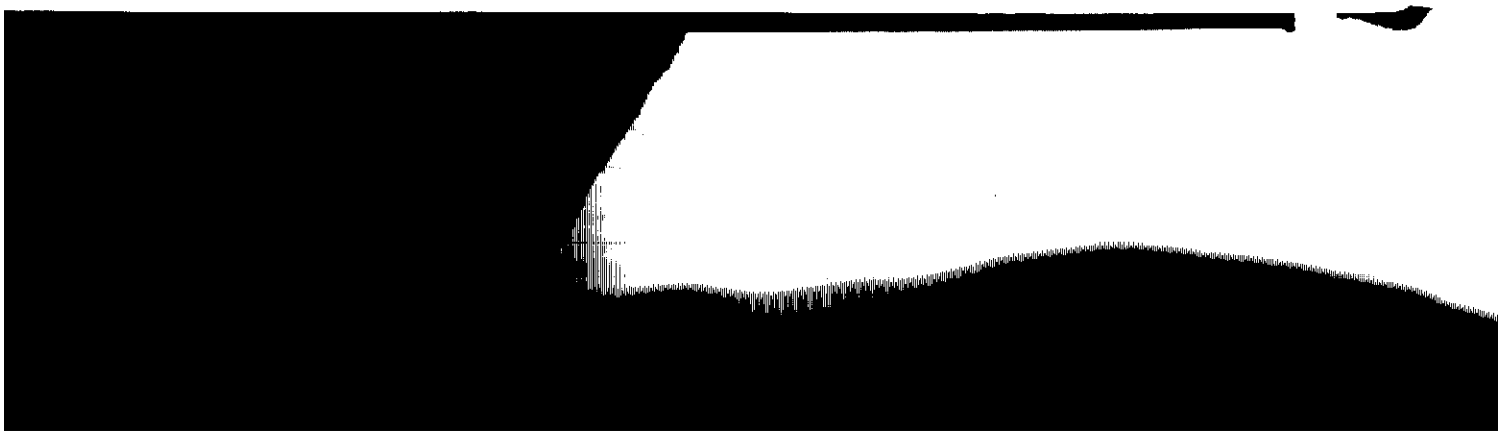

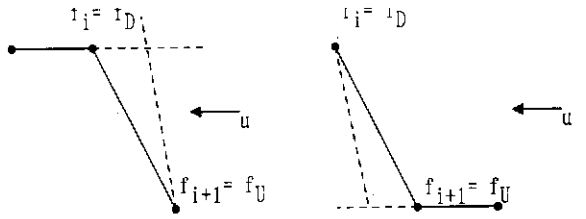

Fig. 2. Special treatment at a discontinuity.

correct interpolations at a discontinuity. As suggested in the previous papers [3,4], one of the improvements can be made by replacing the cubic polynomial by a linear function at NP = ±1. However, the linear function must be carefully chosen. Here we propose a function schematically shown in fig. 2, where a function between f_i and f_{i+1} is approximated by two linear functions. Let us denote the value of f and its spatial derivative as $f_{U(D)}$ and $f'_{U(D)}$. Here the subscripts U and D mean upstream and downstream. Then the value f_i^{n+1} is given by either

$$f_1 = f_U - (\Delta x + u\,\Delta t) f'_U \quad \text{or}$$
$$f_2 = f_D - u\,\Delta t f'_D,$$

where $u < 0$. In the case shown in fig. 2a, it is better to choose $f^{n+1} = \min(f_1, f_2)$. In contrast, if $f_U > f_D$, we choose $f^{n+1} = \max(f_1, f_2)$. For $f_i'^{n+1}$, we choose f'_U (or f'_D) when f_1 (or f_2) is chosen. In the case shown in fig. 2b, we must choose $f^{n+1} = \max(f_1, f_2)$. This choice changes inversely for $u \geq 0$. In any case, however, we understand that we must choose the solution given by the dashed line in the figure. These processes are simply written if we introduce ip. In fig. 2a, f_i is located at the edge and we set ip = 1 there, whereas ip = −1 in fig. 2b because f_i is not at the edge. Thus the procedure is simply written as:

subroutine LINEAR(f_U, f'_U, f_D, f'_D, ip)

$f_1 = f_U - (\Delta x \times \text{isgn} + u\,\Delta t) f'_U$
$f_2 = f_D - u\,\Delta t f'_D$
if $\text{ip} \times (f_D - f_U)(f_2 - f_1) < 0$ *then*
  $f_i^{n+1} = f_2$
  $f_i'^{n+1} = f'_D$
else
  $f_i^{n+1} = f_1$
  $f_i'^{n+1} = f'_U$
endif

(12)

where isgn is as defined in eq. (11). This subprogram is called after the last line of eq. (11). Therefore, we add the following 4 lines after the last line of eq. (11).

if $\text{NP}_i = -\text{isgn}$ *and* $(u_{i+1} - u_{i-1}) \geq 0$ *then*
  call LINEAR($f_{i+\text{isgn}}$, $\text{GP}_{i+\text{isgn},-\text{isgn}}$, f_i, $\text{GP}_{i,-\text{isgn}}$, 1)
if $\text{NP}_{i+\text{isgn}} = \text{isgn}$ *and* $(u_{i+1} - u_{i-1}) \geq 0$ *then*
  call LINEAR($f_{i+\text{isgn}}$, $\text{GP}_{i+\text{isgn},\text{isgn}}$, f_i, $\text{GP}_{i,\text{isgn}}$, −1)

(13)

This interpolation is effective only for constant velocity $u_{i+1} - u_{i-1} = 0$ and for the decompression phase $u_{i+1} - u_{i-1} > 0$. For the compression phase, the gradient becomes steep and hence eq. (13) is of no use.

The result of this latter scheme (we call this CIP2) is given in fig. 1c. Even after 1000 steps, the discontinuity is described exactly as it was initially. In this case, the initial condition for f' is taken to be $f_i' = (f_{i+1} - f_i)/\Delta x$ or $= (f_i - f_{i-1})/\Delta x$, where the one having the larger absolute value is chosen. In contrast, we can set $f_i' = (f_{i+1} - f_{i-1})/2\ \Delta x$. In this case, however, there appears one additional point just in the middle of the discontinuity.

5. Nonlinear problem

Let us consider a hyperbolic equation,

$$\frac{\partial f}{\partial t} + \frac{\partial fu}{\partial x} = g, \tag{14}$$

where the advection velocity u and the source term g can be a function of f. It should be noted that the following discussion can also apply to the case where f is a vector quantity. According to the PIC (particle-in-cell) algorithm [10], we split the above equation into two phases; the nonadvection phase $\partial f/\partial t = G$ and the advection phase $\partial f/\partial t + u\ \partial f/\partial x = 0$. Here we have moved the compression term $f\ \partial u/\partial x$ on the left-hand side of eq. (14) to the right-hand side and have introduced,

$$G = g - f\frac{\partial u}{\partial x}. \tag{15}$$

The compact-CIP solvers that were given in sections 2, 3 and 4 are applied only to the advection phase after the nonadvection phase is solved with a finite-difference approach.

For the spatial derivative of eq. (14), we have

$$\frac{\partial f'}{\partial t} + u\frac{\partial f'}{\partial x} = G' - f'\frac{\partial u}{\partial x}. \tag{14'}$$

This equation is also split into two phases: $\partial f'/\partial t = G' - f'\ \partial u/\partial x$ (nonadvection) and $\partial f'/\partial t + u\ \partial f'/\partial x = 0$ (advection).

We now discuss a method to solve these equations separately for the nonadvection and the advection phases.

5.1. Nonadvection phase

The equation for f, $\partial f/\partial t = G$, is simply solved using finite differencing,

$$f_i^* = f_i^n + G_i\ \Delta t, \tag{16}$$

where * on f means the time after one time step in the nonadvection phase. Even if G includes the diffusion term and must be solved implicitly, the implicit solver can be applied to this phase. We need not convert eq. (14') for f' into a finite-difference form. As has been discussed in our previous paper [2], a simple treatment is possible. The time evolution of f' associated with G' can be estimated from eq. (16). Thus, we approximate the time evolution of f' with the finite difference of the time evolution of f to be

$$\frac{(f_i'^* - f_i'^n)}{\Delta t} = \frac{(f_{i+1}^* - f_{i-1}^* - f_{i+1}^n + f_{i-1}^n)}{2\ \Delta x\ \Delta t}. \tag{17}$$

If we compare this equation with eq. (16), we understand that this is equivalent to

$$\frac{(f_i'^* - f_i'^n)}{\Delta t} = \frac{(G_{i+1} - G_{i-1})}{2\,\Delta x}. \tag{18}$$

However, the great difference is in the universality and simplicity of eq. (17) because f^* is already given and is simply used to estimate the evolution of f'. Equation (18) needs the finite-difference form of G and may not be straightforward when G includes higher-order spatial derivatives and nonlinear terms.

Another term $f'\,\partial u/\partial x$ in eq. (14′) can simply be solved with finite differencing; thus we have

$$\frac{(f_i'^* - f_i'^n)}{\Delta t} = \frac{(f_{i+1}^* - f_{i-1}^* - f_{i+1}^n + f_{i-1}^n)}{2\,\Delta x\,\Delta t} - f_i'^n \frac{(u_{i+1} - u_{i-1})}{2\,\Delta x}. \tag{19}$$

5.2. Advection phase

After f and f' are advanced in the nonadvection phase, the CIP solver is applied to the advection phase. The interpolated profile is determined from eqs. (5)–(8) using f^* and f'^* on the right-hand side.

These two phases complete one time step of the calculation; then after replacing f^{n+1} and f'^{n+1} by f^n and f'^n, we return to the nonadvection phase again.

6. KdV equation

In order to show that both the basic and improved schemes are effective even in nonlinear problems, we first apply the scheme to the KdV equation:

$$\frac{\partial f}{\partial t} + (u + U_d)\frac{\partial f}{\partial x} + \delta^2 \frac{\partial^3 f}{\partial x^3} = 0, \tag{20}$$

where U_d is the constant drift velocity. The procedure for this equation is not very different from the one given in previous sections:

Sequence for the KdV equation

(1) Set initial conditions; $f_i = \sin kx$, $f_i' = k \cos kx$, $u_i = f_i$, $\Delta x = 2/\text{imax}$, imax = 192. The system is periodic in space and hence $f_1 = f_{\text{imax}+1}$.
(2) Δt is controlled by conditions: $u\,\Delta t/\Delta x$ and $\delta^2\,\Delta t/\Delta x^3 < 0.1$ at each time step.
(3) f is advanced with $\delta^2\,\partial^3 f/\partial x^3$ (see eq. (16)).
(4) f' is advanced with eq. (19).
(5) Call CIP(f, f', u), where CIP represents CIP0, CIP1, CIP2.
(6) Repeat (2) to (5).

It is well known that the equation has a shock-like solution for $\delta = 0$ and a solution for a traveling wave train for $\delta \neq 0$. Figure 3 shows two examples of these solutions with CIP0. Figures 3a and 3b are the results for $U_d = 0$, and $\delta = 0$ and $\delta = 0.022$, respectively. The initial profile is shown by the solid line. The profiles shown by the dots are those at $t = 1.6/\pi$ for $\delta = 0$ and $t = 3.6/\pi$ for $\delta = 0.022$. These results are almost the same as those obtained with CIP1 and CIP2. It is surprising that the shock structure for $\delta = 0$ is described by only one mesh without any numerical oscillations even with CIP0. There exist some schemes which can treat the latter case ($\delta = 0.022$) better than the present one. However, they cannot treat the

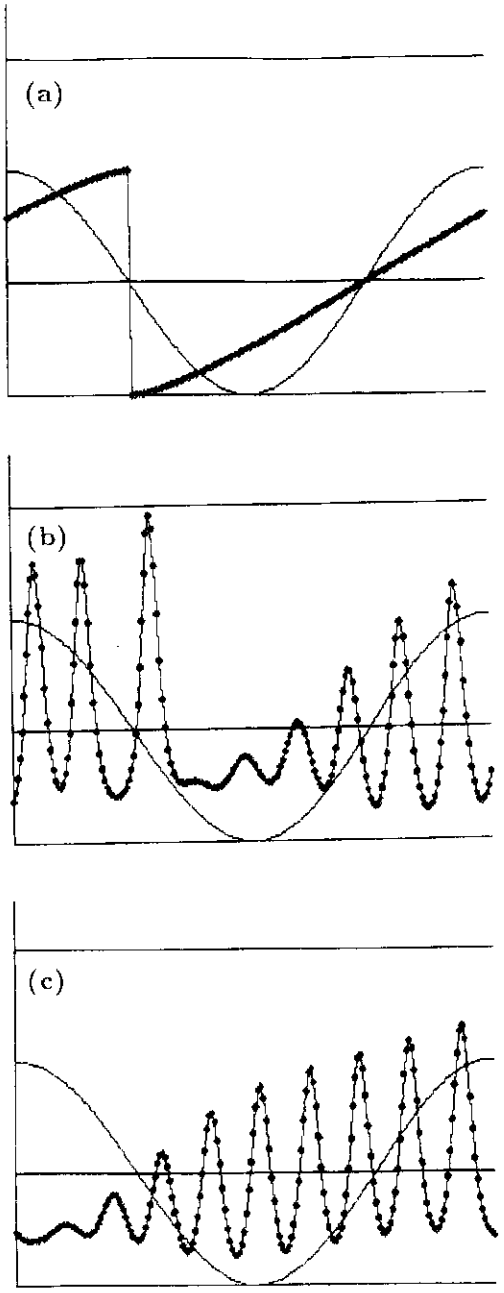

Fig. 3. Solutions of the KdV equation with CIP0. (a) $\delta = 0$, $U_d = 0$, (b) $\delta = 0.022$, $U_d = 0$ and (c) $\delta = 0.022$, $U_d = 3$.

former case ($\delta = 0$) in turn. The solution for $\delta = 0.022$ and $U_d = 3$ is shown in fig. 3c. This case is relatively hard to track, because the numerical diffusion is usually proportional to the advection velocity, and it will dissipate the travelling wave train. Analytically, the amplitude of the wave train in fig. 3b should be the same as that in fig. 3c, but there is a phase lag of about π between the two figures because of U_d.

7. Hydrodynamic equations in planar geometry

Although artificial viscosity is not included in the KdV equation, it must be added when the equation consists of many coupled quantities such as mass, momentum and energy conservation, as do hydrodynamic equations, for instance. We may expect a further advancements in solving the problem in the future. Although the scheme is incomplete in this sense, we suggest a procedure to attack these hydrodynamic equations:

$$\frac{\partial \rho}{\partial t} + \frac{\partial \rho u}{\partial x} = 0, \tag{21}$$

$$\frac{\partial u}{\partial t} + u\frac{\partial u}{\partial x} = -\frac{1}{\rho}\frac{\partial p}{\partial x}, \tag{22}$$

$$\frac{\partial e}{\partial t} + u\frac{\partial e}{\partial x} = -\frac{p}{\rho}\frac{\partial u}{\partial x}, \tag{23}$$

where ρ is the density, u the velocity, p the pressure, and e the specific internal energy.

These equations are split into two phases as shown in the previous section. If we remember that $\boldsymbol{f}$ and $\boldsymbol{g}$ are vectors in eq. (14), eqs. (21)–(23) can be rewritten as

$$\frac{\partial \boldsymbol{f}}{\partial t} + u\frac{\partial \boldsymbol{f}}{\partial x} = \boldsymbol{G}, \tag{24}$$

by using

$$\boldsymbol{f} = (\rho, u, e), \qquad \boldsymbol{G} = \left(-\rho\frac{\partial u}{\partial x}, -\frac{1}{\rho}\frac{\partial p}{\partial x}, -\frac{p}{\rho}\frac{\partial u}{\partial x}\right). \tag{25}$$

Here we discuss an approach that uses staggered meshes to solve these equations. First, we describe a solution in a staggered mesh system; that is, ρ, p and e are defined at the grid point x_i and u is defined at $x_{i+1/2}$. The finite-difference forms in the nonadvection phase are then given by

$$\frac{\rho_i^* - \rho_i^n}{\Delta t} = -\rho_i^n\frac{u_{i+1/2}^n - u_{i-1/2}^n}{\Delta x}, \tag{26}$$

$$\frac{u_{i+1/2}^* - u_{i+1/2}^n}{\Delta t} = -\frac{2}{\rho_{i+1}^n + \rho_i^n}\frac{p_{i+1}^n - p_i^n}{\Delta x}, \tag{27}$$

$$\frac{e_i^* - e_i^n}{\Delta t} = -\frac{p_i^n}{\rho_i^n}\frac{u_{i+1/2}^* - u_{i-1/2}^* + u_{i+1/2}^n - u_{i-1/2}^n}{2\,\Delta x}. \tag{28}$$

Therefore, the procedure to solve hydrodynamic equations is given by:

Sequence for 1-D hydrodynamic equations

(1) Set initial conditions.
(2) Get ρ^*, u^*, e^* from eqs. (26)–(28).
(3) Get ρ'^*, u'^*, e'^* from eq. (19).
(4) Use CIP to get ρ^{n+1}, ρ'^{n+1}, u^{n+1}, u'^{n+1}, e^{n+1}, e'^{n+1}: call CIP (ρ^*, ρ'^*, u_{av}), call CIP (u^*, u'^*, u), and call CIP (e^*, e'^*, u_{av}). (Here, the advection velocity for ρ^* and e^* is taken to be $u_{\mathrm{av}} = (u_{i+1/2}^* + u_{i-1/2}^*)/2$.)
(5) Repeat (2) to (4).

latively
l it will
be the

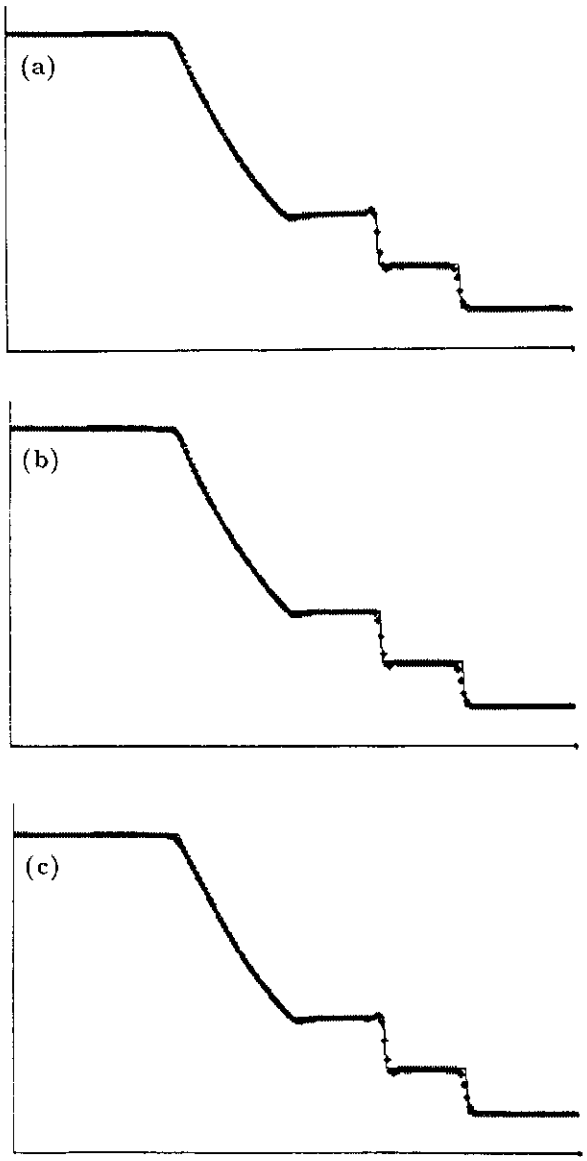

Fig. 4. Shock-tube problem. Initial conditions: $\rho = 1$, $u = 0$, $p = (\gamma - 1)e = 1$ for $0 \le x \le 1$ and $\rho = 0.125$, $u = 0$, $p = 0.1$ for $1 < x \le 2$, where $\Delta x = 0.01$, $\Delta t = 0.001$ and $\gamma = 1.4$. A profile at $t = 0.276$ is shown. (a) CIP0, (b) CIP1 and (c) CIP2.

This scheme is tested with a typical shock-tube problem [2]. A result for CIP0 is shown in fig. 4a. Here, we have added the numerical viscosity q_i to the pressure term as shown in ref. [10],

$$q_i = a\left(-\rho_i C_a\, \Delta u + \frac{\gamma+1}{2}\rho_i\, \Delta u^2\right) \quad \text{if} \quad \Delta u < 0,$$
$$= 0 \quad \text{if} \quad \Delta u \ge 0, \tag{29}$$

where C_a is the sound velocity and $\Delta u = u_{i+1/2} - u_{i-1/2}$. In this case, $a = 0.6$–0.75 has been used. In all the calculations for shock waves, we have used $a = 0.75$. In fig. 4a, both the shock wave and the contact

discontinuity are described with one or two meshes. The results for CIP1 and CIP2 are shown in figs. 4b and 4c, respectively. Surprisingly, the result for CIP0 is not very different from those for the improved schemes.

The CIP method treats contact discontinuities better than other methods reviewed by Sod [11] and TVD schemes given by Yee [12] as well as shock fronts. The CIP scheme belongs to explicit artificial viscosity (EAV) schemes, whereas most of the modern schemes belong to implicit artificial viscosity (IAV) schemes. The EAV becomes advantageous in some cases because it can control the magnitude of the viscosity. This is clearly seen in one-fluid and two-temperature models frequently used in plasma physics. Since electron viscosity is much smaller than ion viscosity by a factor of the square root of the mass ratio, the electron temperature evolves according to adiabatic law even at shock fronts. The EAV can treat this problem by suppressing AV in electron energy equation. A detailed discussion on this problem will be given in the future.

In some cases, the staggered mesh becomes difficult to apply. Even such a case, we can modify the above scheme to a nonstaggered mesh system, where all the quantities are defined at the same point x_i and eq. (27) is modified to be

$$\frac{u_i^* - u_i^n}{\Delta t} = -\frac{1}{\rho_i^n}\frac{p_{i+1/2}^n - p_{i-1/2}^n}{\Delta x}, \tag{27'}$$

other equations ((26) and (28)) being unchanged. Thus, we need to estimate the quantities such as $p_{i\pm1/2}$. Taking an average $p_{i+1/2} = (p_{i+1} + p_i)/2$ is not as good as the method proposed here. The coupling between meshes in this averaging scheme is weak, and small oscillations frequently occur when it is used [3].

We can estimate the value at $i \pm 1/2$ with the cubic-interpolated profile since we have already chosen a profile given by eq. (3). Therefore, the procedure to solve hydrodynamic equations is similar to that for the staggered mesh system. The only difference is that eq. (27') is used and step (1') is added between steps (1) and (2) to obtain the value of ρ, p, u at $i \pm 1/2$ from eq. (3) setting $X = \Delta x/2$. In step (4), we need not use u_{av} but simply use u for the calculation of ρ and e. The result using this scheme is not very different from that in a staggered mesh system and will not be discussed in detail here.

8. Hydrodynamic equations in other geometries

The scheme in plane geometry can easily be extended to other geometries. Then eqs. (21)–(23) can be rewritten as

$$\frac{\partial \rho}{\partial t} + \frac{1}{r^\delta}\frac{\partial \rho u r^\delta}{\partial r} = 0, \tag{30}$$

$$\frac{\partial u}{\partial t} + u\frac{\partial u}{\partial r} = -\frac{1}{\rho}\frac{\partial p}{\partial r}, \tag{31}$$

$$\frac{\partial e}{\partial t} + u\frac{\partial e}{\partial r} = -\frac{p}{\rho r^\delta}\frac{\partial u r^\delta}{\partial r}, \tag{32}$$

where δ is 0, 1 and 2 for planar, cylindrical and spherical geometry, respectively, giving

$$G = \left(-\frac{\rho}{r^\delta}\frac{\partial r^\delta u}{\partial r}, -\frac{1}{\rho}\frac{\partial p}{\partial r}, -\frac{p}{\rho r^\delta}\frac{\partial r^\delta u}{\partial r}\right).$$

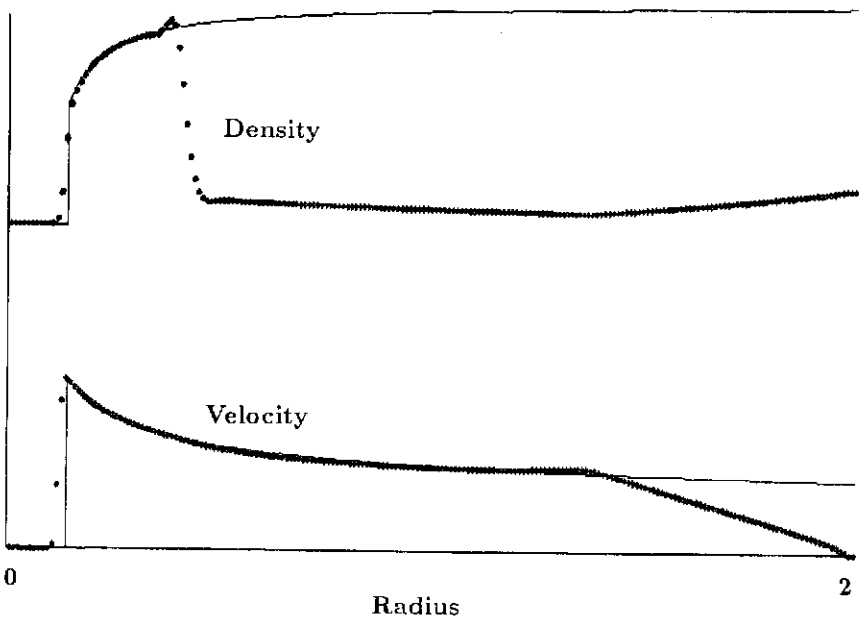

Fig. 5. Cylindrically converging shock wave. Density (top figure) and velocity (bottom figure) profiles obtained with CIP0 at $t = 80$ are shown by dotted lines; solid lines show the self-similar solution.

Thus, only eqs. (26) and (28) in the nonadvection phase are changed, whereas the advection phase remains unchanged. In addition to this, $u_{i+1} - u_{i-1} \geq 0$ in eq. (13) must be changed to $(r^\delta u)_{i+1} - (r^\delta u)_{i-1} \geq 0$. A similar argument applies also to Δu in eq. (29).

In fig. 5, we show an example of a cylindrically converging shock wave obtained with CIP0. The solid line shows a self-similar solution described in the appendix, and the dotted line shows the numerical result. The numerical solution deviates from the self-similar solution at and outside the contact surface. This is due to the initial conditions used here: initially, $\rho = 0.5$, $u = 0$, $p = (\gamma - 1)e = 0$ for $0 \leq x < 100$ and $\rho = 1$, $u = 0$, $p = 1$ for $100 \leq x \leq 200$, where $\Delta x = 1$ and Δt is determined from the CFL number ($= 0.2$), and $\gamma = \frac{5}{3}$. As is predicted from the results in section 7, the results with the improved schemes are not very different from the result shown in fig. 5.

9. Summary

We have developed a new universal hyperbolic solver. The method need not solve the Rieman problem and hence can straightforwardly be applied to a variety of problems. Many different kinds of equations, such as the KdV equation and hydrodynamic equations in planar and cylindrical geometries, are solved with the same subroutine as is used for the advection process. The nonadvection term is treated simply with a finite-difference method.

Shock waves and solitary waves were successfully traced with high accuracy. The shock front and contact discontinuity were described with a few meshes without serious overshooting. From these results, we conclude that the basic scheme CIP0 can give sufficient results in almost all nonlinear problems, and the improved schemes CIP1 and CIP2 give similar results for those problems. In particular the latter two are effective for linear advection when extremely high resolution is required. The reason why the CIP method works so well is still not clear and detailed investigation of the characteristics is an interesting future subject.

This one-dimensional solver can also be used for multidimensional cases with a time-splitting technique [2,4]. However, direct extension of the compact CIP is possible [13] without time splitting. This problem will be discussed in part II of this series of papers.

Appendix. Self-similar solution

In the absence of heat conduction, viscosity and other nonhydrodynamic processes, hydrodynamic equations are generally written as

$$\frac{\partial \rho}{\partial t} + \frac{\partial \rho}{\partial r} + \frac{\delta \rho u}{r} = 0, \tag{A.1}$$

$$\frac{\partial u}{\partial t} + u\frac{\partial u}{\partial r} = -\frac{1}{\rho}\frac{\partial p}{\partial r}, \tag{A.2}$$

$$\frac{\partial p\rho^{-\gamma}}{\partial t} + u\frac{\partial p\rho^{-\gamma}}{\partial r} = 0, \tag{A.3}$$

where δ is the geometrical factor and is 0, 1, and 2 for planar, cylindrical, and spherical geometry, respectively. We transform the variables to

$$\rho = \rho_0 r^k F(\xi), \tag{A.4}$$

$$u = (r/t)V(\xi), \tag{A.5}$$

$$\gamma p/\rho = (r/t)^2 Z(\xi), \tag{A.6}$$

introducing

$$\xi = rt^{-a}, \tag{A.7}$$

With tedious calculations, we finally reach the form [14]:

$$\frac{\mathrm{d}V}{\mathrm{d}(\ln \xi)} + (V-a)\frac{\mathrm{d}(\ln F)}{\mathrm{d}(\ln \xi)} = -(k+\delta+1)V, \tag{A.8}$$

$$(V-a)\frac{\mathrm{d}V}{\mathrm{d}(\ln \xi)} + \frac{Z}{\gamma}\frac{\mathrm{d}(\ln F)}{\mathrm{d}(\ln \xi)} + \frac{1}{\gamma}\frac{\mathrm{d}Z}{\mathrm{d}(\ln \xi)} = -\frac{(2+k)}{\gamma}Z - V(V-1), \tag{A.9}$$

$$(\gamma-1)Z\frac{\mathrm{d}(\ln F)}{\mathrm{d}(\ln \xi)} - \frac{\mathrm{d}Z}{\mathrm{d}(\ln \xi)} = \frac{[k(1-\gamma)+2]V-2}{V-a}Z. \tag{A.10}$$

Let us consider a situation where a shock wave propagates towards the center through a uniform ($k = 0$) media in a cylindrical geometry ($\delta = 1$). If we measure the time from $-\infty$ to 0 (0 means the time of collapse), the boundary condition that may be considered is that at the center, $r = 0$. This will not put any restriction on the exponent a. This is also true for the shock wave front. The jump condition at the shock front is written as

$$F(\xi_s) = \frac{\gamma+1}{\gamma-1}, \qquad V(\xi_s) = \frac{2}{\gamma+1}a, \qquad Z(\xi_s) = \frac{2\gamma(\gamma-1)}{(\gamma+1)^2}a^2. \tag{A.11}$$

In eq. (A.11), the location of a shock wave is given by $\xi = \xi_s = r/t^a = \text{constant}$. From this relation, the velocity of the shock wave C_s is given by $C_s = \mathrm{d}r/\mathrm{d}t = ar/t$.

Rearranging eqs. (A.8)–(A.10), we obtain

$$\frac{dZ}{d(\ln \xi)} = \frac{Z\Delta_Z}{(V-a)\Delta}, \frac{dV}{d(\ln \xi)} = \frac{\Delta_V}{\Delta}, \tag{A.12}$$

where

$$\Delta = (V-a)^2 - Z, \tag{A.13}$$

$$\Delta_V = -V(V-1)(V-a) + Z[(\delta+1)V+\beta], \tag{A.14}$$

$$\Delta_Z = -(V-a)^2[2(V-1)+(\gamma-1)(\delta+1)V] + (\gamma-1)V(V-1)(V-a) + Z[2(V-1)-\beta(\gamma-1)], \tag{A.15}$$

$$\beta = [a(k+2)-2]/\gamma. \tag{A.16}$$

From eqs. (A.12) and (A.13), the solution becomes singular when the denominator vanishes, that is $\Delta = 0$. This occurs on the parabola

$$Z = (V-a)^2 \tag{A.17}$$

in the Z–V plane. In order for a finite solution to exist, the numerators in eq. (A.12), that is Δ_V and Δ_Z, should vanish simultaneously. Since three conditions, eq. (A.17), $\Delta_V = 0$, and $\Delta_Z = 0$ must be satisfied, two variables Z and V are not sufficient, and hence the solution exists only for a specific value of a.

The values of a for various γ and δ have been calculated numerically and are given in ref. [14]. For $\gamma = \frac{5}{3}$ and $\delta = 1$, $a = 0.815625$. We solve eqs. (A.12) and (A.8) from the shock front (A.11). We define the shock front as $\xi_s = 1$ and hence eq. (A.7) becomes

$$\xi = \frac{r}{A(t_c - t)^a}, \tag{A.7'}$$

where t_c is the collapse time of the shock wave at the center. The constant A is calculated from the initial radius r_0 by setting $\xi_s = 1$ and $r = r_0$, $t = 0$ in eq. (A.7').

$$A = r_0 t_c^{-a}.$$

In the example shown in fig. 5, $r_0 = 100$ and $t_c = 88$.

References

[1] H. Takewaki, A. Nishiguchi and T. Yabe, J. Comput. Phys. 61 (1985) 261.
[2] H. Takewaki and T. Yabe, J. Comput. Phys. 70 (1987) 355.
[3] T. Yabe and E. Takei, J. Phys. Soc. Japan 57 (1988) 2598.
[4] T. Yabe, P.Y. Wang and G. Sakaguchi, in: Proc. Int. Conf. Computational Fluid Dynamics, Nagoya, Japan, August 1989.
[5] G. Knorr and M. Mond, J. Comput. Phys. 38 (1980) 212.
[6] M.M. Shouri, J. Comput. Phys. 49 (1983) 334.
[7] B. van Leer, J. Comput. Phys. 32 (1979) 101.
[8] A. Harten, SIAM J. Numer. Anal. 21 (1984) 1.
[9] P. Colella and P.R. Woodward, J. Comput. Phys. 54 (1984) 174.
[10] A. Nishiguchi and T. Yabe, J. Comput. Phys. 52 (1983) 390.
[11] G.A. Sod, J. Comput. Phys. 27 (1978) 1.
[12] H.C. Yee, NASA Report TM-89464 (1987).
[13] T. Yabe, T. Ishikawa, Y. Kadota and F. Ikeda, J. Phys. Soc. Japan 59 (1990) 2301.
[14] Y.B. Zel'dovich and Y.P. Raizer, Physics of Shock Waves and High-Temperature Hydrodynamic Phenomena, vol. II (Academic, New York, 1967).
[15] T. Yabe, T. Ishikawa, P.Y. Wang, T. Aoki, Y. Kadota and F. Ikeda, Comput. Phys. Commun. 66 (1991) 233, this issue.